2022 IEEE International Conference on Cyborg and Bionic Systems
March 24-26, 2023, Wuhan, China

2022 IEEE International Conference on Cyborg and Bionic Systems (CBS) | 978-1-6654-9028-3/23/$31.00 ©2023 IEEE | DOI: 10.1109/CBS55922.2023.10115390

# Underwater Image Enhancement based on Improved Water-Net

Yuhan Chen[1], Huazhong Li[2], Quande Yuan[3], Zhen Wang[1], Chengzhi Hu[1], Wende Ke[1*]

*Abstract* — **Enhancement for underwater image has been gradually valued with the development of ocean engineering as well as remote operated vehicles. Multifarious methods are applied in underwater image enhancing recently. Particularly, varieties of convolutional neural networks (CNN) have been applied for this field. However, during distrinct conditions lightness and medium quality, underwater images are complex and variable, which makes it much more challenging for CNN models to enhance images in different environments. In this paper, improvements are made to the architecture in Water-Net, in which we increased the enhancement units (E-Units) in the backbone of the network and improved the output of the confidence map. Experimental results on Underwater Image Enhancement Benchmark (UIEB) indicate that our network achieved better capability than other algorithms.**

*Keywords* — **neural network, image enhancement, enhancement unit**

## I. INTRODUCTION

Recently, ocean exploitation, underwater detection, environment conservation and marine military developed swiftly and have gradually attracted people's attention to underwater image technology. As an essential part of underwater image technology, many researchers have engaged in underwater image enhancement [1-3]. Multivariate ambient condition and differnt light spreading make enhancement in underwater environment a large challenge [4]. In the earlier stage, image enhancement was often achieved through information fusion, which used multiple sensors for image processing and correction[5-8]. However, underwater image enhancement with a single visual sensor not only saves hardware costs but is also more helpful for adapting to complex underwater environments. Thus the upgrading focus on enhancing underwater information has gradually changed from equipment improvement to breakthrough in algorithms.

There are two main ideas for traditional underwater image enhancement methods. One is based on uncomplicated mathematical, the other treat the enhancement as physical problems. Uncomplicated mathematical based algorithms improved anthropic visual quality by modifying channel values in pixels according to several mathematical and statistical equations. In the original study of uncomplicated mathematical methods, color-balance [9-10], histogram balance [11-13] as well as non-linear correction [14-15] methods have been adapted. Besides, channel values in HSV color space [16] was also used in improving saturation and hue of underwater images. Inspired by architecture of teleost fishes' retina, a larruping enhancing algorithm was proposed [17], the introduction of HSV eliminated degradation caused by mistiness and heterogeneous color cast. Other researchers in uncomplicated mathematical methods tried to make enhancements according to Retinex model[18-20]:

$$S(i,\ j) = L(i,\ j) \cdot R(i,\ j) \tag{1}$$

$S(i, j)$ represents pixel value of $(i, j)$ in visual sensor imaging, $L(i, j)$ denotes incident light intensity in pixel $(i, j)$, and $R(i, j)$ denotes reflect light intensity of the object. Physics-based methods thinks of restoration for underwater images as inverse problems, where the latent parameters of physical models are evaluated from known conditions. Plenty of physics-based methods are established on dark channel prior (DCP) mechanism [21]:

$$I_\lambda(i,\ j) = J_\lambda(i,\ j) \cdot t(i,\ j) + A_\lambda \cdot (1 - t(i,\ j)) \tag{2}$$

where $I_\lambda(i, j)$ denotes pixel in observer vision, $J(i, j)$ indicates the pixel in corresponding groundtruth, $t(i, j)$ represents transmission map pixel value, and $A_\lambda$ represents background light. The deblurring objective is estimating $J_\lambda(i, j)$ according to $I_\lambda(i, j)$ free from $A_\lambda$ and $t(i, j)$. In [22], a novel DCP model was put forward in consideration of red channel values from underwater images are not dependable. Later on, Generalized GDCP [23] was introduced and fused self-adaption adjustment during the enhancement.

With the development of computer and artificial intelligence, neural network gradually took part in underwater image technology, which brings many breakthroughs in underwater image enhancement. Plenty of neural networks are established for enhancing underwater images and some of them are based on CNNs [4], [20], [24-27] others are based on GANs [28-31]. CNN models were established to make enhancement from raw images, while the aim of GAN models are to raise perceptual quality of the whole underwater images. Nevertheless, application of neural networks in underwater image processing is difficult due to the complex and

*This work is supported by Project of Guangdong education bureau: the graduate training of government, university and enterprise by Southern University of Science and Technology - Leju (Shenzhen) Robotic Corporation, the Science and Technology Development Plan Project of Jilin Province (Grant No. 20210201049GX), Shenzhen basic research project (JCYJ20180307124010740), School level scientific research project of Shenzhen Institute of information technology (SZIIT2020KJ016,XQ202026 , LHPY-2020007，LHPY-2020008). This work is supported in part by the Science, Technology and Innovation Commission of Shenzhen Municipality under grant no. ZDSYS20200811143601004, and in part by the Southern Marine Science and Engineering Guangdong Laboratory (Guangzhou).

Author affiliations: (1) Y. Chen, Z. Wang, C. Hu, W. Ke are from Southern University of Science and Technology, Shenzhen, China, 518055. (2) H. Li is from Shenzhen Institute of Information Technology, Shenzhen, China, 518172. (3) Q. Yuan is from Changchun Institute of Technology, Changchun, China, 130012 (corresponding email: kewd@sustech.edu.cn).

changeable environmental factors such as light and water quality.

Our contributions in this paper are summarized below:

- Improved Water-Net (IWNet) was proposed in which we changed the original structure of Water-Net[4] from a series to several enhancement units (E-Units). These E-Units obtain high quality underwater images while holding the texture characteristics of raw images, which sloved the problem of image distoration caused by networks too deep [24].
- Correct output values of the confidence map values by Softmax. Let the sum of confidence map values be constant so that the output values can be obtained within a certain range. With this improvement, our model achieves more stable results on underwater image benchmark.

## II. Related Work

### A. Neural network based underwater image enhancement

Nowadays, neural network was amply applied in various kinds of visual tasks due to its strong feature learning ability, and has achieved extremely competitive performance. Li et al. [24] introduced an under water convolutional neural network (UWCNN), the network consists of three E-Units. However, UWCNN was separated from the end-to-end approaches, and the architecture of UWCNN is relatively simple. The enhancing results from UWCNN models are not perfect. Water-Net [4] was proposed later, where Water-Net is mixed with three mathematical based methods through CNN. However, the traditional chain architecture can not completely retain pristine features of images. In 2021, an enhancement network with RGB and HSV channels (UICE^2-Net) [25] came into being, UICEˆ2-Net appropriately integrated both RGB and HSV colour spaces into a simple neural network, which achieved underwater image enhancement results very well.

### B. Underwater image dataset

It is obvious that underwater image enhancement based on neural networks are supposed to be trained in datasets with large amount of images. A data set for underwater enhancing in real world (RUIE) [32] was born from Dalian University of Technology, which is characterized by a large amount of data, diverse degrees of light scattering effects, rich colors, and rich detection targets, RUIE can easily measure performance of enhancing algorithms from multiple perspectives, such as visibility enhancement, color bias correction, and task drive. Berman et al. [33] proposed Stereo Quantitative Underwater Image Dataset (SQUID). The images in the dataset were collected from various water quality and water depth below, and color charts were applied for enhancement evaluation. In addition, the stereoscopic scene was rebuilt according to RGB-D information. Thus objective evaluations of reduction algorithms on natural images is available in SQUID. Later on, a novel underwater enhancement data set (UIEB) [4] was provided by Tianjin University, which consists of a basic dataset and a challenging dataset, the basic dataset inaclding 890 underwater images as well as corresponding references. Reference images in the dataset are obtained by raw images processed in different algorithms and manual selected.

## III. Proposed Model

During section III, we expound network architecture of our proposed IWNet at first, and then introduce loss functions applied in IWNet.

### A. Global structure and details

Improved Water-Net is a novel model with convolutional layers in series, as shown in Figure 1, which consists of three kinds of E-Units shown in Figure 2 and one Global Softmax unit shown in Figure 3. Similar to the Water-Net, our proposed network gated fuses inputs of three traditional processed results with the estimated confidence maps to obtin output enhancement results.

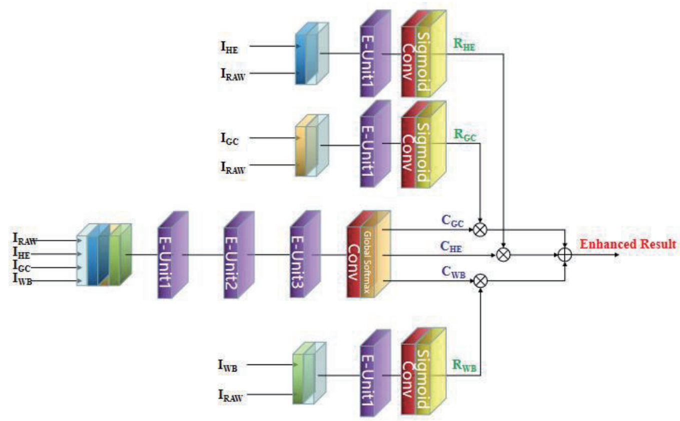


Figure 1. Improved Water-Net backbone structure.

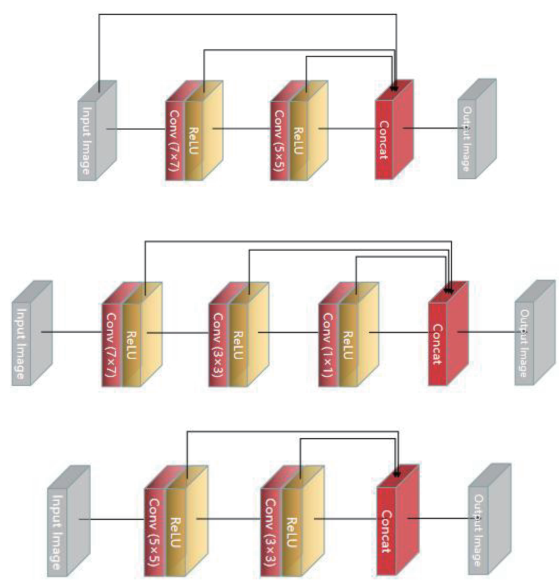


Figure 2. Structure of E-Units. (a) Structure of E-Unit1. (b) Structure of E-Unit2. (c) Structure of E-Unit3.

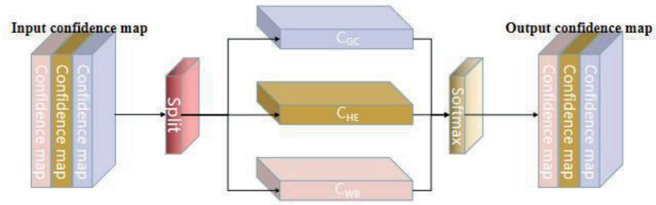


Figure 3. Structure of Global Softmax.

**Enhancement Units:** Take a simple improvement from the structure of the original Water-Net, and change the simple baseline model to the combination of some Enhancement Units (E-Units). The E-Units are in three different structures. Set *r* as ReLU transformation and *c* as convolution procession, *h* means concat layer with dimension=3. $U_0$ is the input that concatenates raw images, images preliminarily enhanced from histogram balance (HE), non-linear correction (GC) as well as colour balance (WB) along the third dimension of each individual part, $z_{kl}$ represents output of the $l^{th}$ computing process in $k^{th}$ E-Unit, $\theta_{ij}$ represents corresponding parameters. Then the output $b_1$ of E-Unit1 in the confidence map baseline is calculated as follows:

$$\begin{cases} z_{11} = r(c(U_0);\theta_{11}) \\ z_{12} = r(c(z_{11});\theta_{12}) \\ b_1 = h(U_0; z_{11}; z_{12}) \end{cases} \tag{3}$$

The output $b_2$ of E-Unit2 in the confidence map baseline is calculated as follows:

$$\begin{cases} z_{21} = r(c(b_1);\theta_{21}) \\ z_{22} = r(c(z_{21});\theta_{22}) \\ z_{23} = r(c(z_{22});\theta_{23}) \\ b_2 = h(z_{21}; z_{22}; z_{23}) \end{cases} \tag{4}$$

The output $C_0$ of E-Unit3 in the confidence map baseline is calculated as follows:

$$\begin{cases} z_{31} = r(c(b_2);\theta_{31}) \\ z_{32} = r(c(z_{31});\theta_{32}) \\ C_0 = h(z_{31}; z_{32}) \end{cases} \tag{5}$$

The output of HE, GC, WB parts $b_{HE}$, $b_{GC}$, $b_{WB}$ are calculated as follows:

$$\begin{cases} z_{l1} = r(c(U_l);\theta_{l1}) \\ z_{l2} = r(c(U_l);\theta_{l2}) \\ R_l = h(U_l; z_{l1}; z_{l2}) \end{cases} \tag{6}$$

In which *l* means HE, GC or WB, $U_l$ is the input of HE, GC, WB parts:

$$U_l = h(I_{RAW}; I_l) \tag{7}$$

**Output part:** In order to obtain a stable output image, we process the confidence map by the Global Softmax unit. While the confidence map is split into three parts as $C_{HE}$, $C_{GC}$, and $C_{WB}$, which means confidence map parts for triditional algorithms such as HE, GC and WB, we modify the three parts using the Softmax function:

$$C'_l(c,i,j) = \frac{exp(C_l(c,i,j))}{\sum exp(C_l(c,i,j))} \tag{8}$$

where *l* represents HE, GC or WB, c means the three channels of the image, *(i, j)* represents a certain pixel point. Thus the value of each element in the confidence map satisfies:

$$C'_{HE}(c,i,j) + C'_{GC}(c,i,j) + C'_{WB}(c,i,j) = 1 \tag{9}$$

Ultimately, the trained confidence maps are multiplied with three corresponding inputs respectively and the output image is obtained [1]:

$$\hat{I} = R_{WB} \otimes C_{WB} + R_{HE} \otimes C_{HE} + R_{GC} \otimes C_{GC} \tag{10}$$

$\hat{I}$ represents output image; $\otimes$ represents matrices' production by element which satisfies:

$$\begin{aligned} & M = R \otimes C \Leftrightarrow \\ & \forall c,i,j \in \{(c,i,j) \mid \exists M(c,i,j)\}, M(c,i,j) = R(c,i,j) \times C(c,i,j) \end{aligned} \tag{11}$$

where $M(c,i,j)$ means value of channel *c* in pixel *(i,j)*.

## B. Loss function

Our proposed IWNet contains loss function with two loss components. The particular computing process is shown in Equation 12:

$$L = \lambda_{l_1}\omega_{l_1}L_{l_1} + \lambda_{SSIM}\omega_{SSIM}L_{SSIM} \tag{12}$$

where $L_{l1}$ and $L_{SSIM}$ are L1 loss and SSIM loss, respectively, $\lambda_{l1}$, $\lambda_{SSIM}$ are their hyperparameters and $\omega_{l1}$, $\omega_{SSIM}$ are weight hyperparameters. Functions of L1 loss and SSIM loss are evaluated below:

**SSIM loss** [34]**:** This is a novel loss term applied to evaluate appearance similarity between the predicted image from our proposed method and reference image. We compute SSIM in each pixel *(i,j)* within an 11×11 squareness around the pixel, as shown in Equation 13:

$$SSIM(i,j) = \frac{2\mu_I(i,j)\mu_{\hat{I}}(i,j) + c_1}{\mu_I^2(i,j) + \mu_{\hat{I}}^2(i,j) + c_1} \cdot \frac{2\sigma_{I\hat{I}}(i,j) + c_2}{\sigma_I^2(i,j) + \sigma_{\hat{I}}^2(i,j) + c_2} \tag{13}$$

$\mu_{I'}(i,j)$, $\sigma_{I'}(i,j)$ represent the average value and square root error of output results' channel values respectively. Likewise, $\mu_I(i,j)$, $\sigma_I(i,j)$ represent values in the raw image. Besides, $\sigma_{II'}(x)$ represents cross square root error. $c_1$, $c_2$ are set to 0.02 and 0.03 respectively. This loss term evaluated like Equation 14:

$$L_{SSIM} = 1 - \frac{1}{N}\sum_{i=1}^{N} SSIM(x_i) \tag{14}$$

**L1 loss:** This term is used for computing Manhattan error on pixels from IWNet predicted images and ground truth images. The L1 loss is expressed by following Equation 15:

$$L_{l1} = \left\| \hat{I}_i - I_i \right\|_1 \tag{15}$$

**Loss term weights:** We set $\omega_{l1}$=2, $\omega_{SSIM}$=1, $\lambda_{SSIM}$=*1*, and at the first 50 epochs, we set $\lambda_{l1}$=1, and set $\lambda_{l1}$=2 for the last epochs.

# IV. Experimental Results

We apply subjective analysis and objective analysis in enhancement performance validation and contrast proposed network with three traditional algorithms as well as three CNN-based methods. The control group including Histogram Balance (HB), Colour Balance (CB), Non-linear Correction (NC), UWCNN [24], Water-Net [4], UIEC^2-Net [25]. In this section, implementation details will be mentioned at first and then we will make subjective analysis and objective analysis of underwater image enhancement results.

*A. Implementation Details*

Randomly choose 800 underwater images as well as corresponding reference images from UIEB [4] for training set. Raw images will be firstly adjusted into 350×350 and randomly cutted into 320×320 in random. Remaining 90 images as well as corresponding references are applied for evaluating. Input testing images are not unnecessary to be resized or cropped. In addition, we applied ADAM to train constructed program. Then learning rate is initialized as lr = $1e^{-3}$ and reduced as lr' = lr - $1e^{-6}$ in each 100 iteration, and we set the epoch to 100. Pytorch as well as anaconda are assorted with Nvidia GTX 2080Ti GPU for program working.

*B. Quantitative Evaluation*

The testing set, including 90 pairs of images, is used for quantitative analysis. We choose Structural SIMilarity index (SSIM) [35], Mean Square Error (MSE) as well as Peak Signal to Noise Ratio (PSNR) between processed outputs from various algorithms and reference images as our quantitative evaluation to evaluate the enhanced results from above mentioned algorithms. Objective evaluation result as shown in Table 1.

Table 1. Objective evaluation for various algorithms

| **Algorithm** | **MSE** | **PSNR(dB)** | **SSIM** |
|---|---|---|---|
| Inputs | 1501.5072 | 18.4240 | 0.8394 |
| HB | 1029.7292 | 19.3792 | 0.8785 |
| CB | 736.5392 | 23.3571 | 0.9065 |
| NC | 1425.6341 | 17.8363 | 0.8297 |
| UWCNN[24] | 1074.2489 | 20.2142 | 0.8846 |
| Water-Net[4] | 682.5668 | 22.4041 | 0.9221 |
| UIEC^2-Net[25] | 575.0522 | 22.0505 | 0.9238 |
| IWNet | 464.2417 | 24.1423 | 0.9383 |

The quantitative contrasting result states the proposed network has perfect results better than the classical enhancement algorithms and other convolutional neural network based enhancement methods.

*C. Qualitative Evaluation*

As light propagating in underwater environment, red light dissolves firstly, later on green light dissolves, and blue light lastly. Thus majority of images from water are partial to cold tone such as turquoise blue. Besides, some images from seafloor are in low-brightness or tend to be yellow. Enhancing results of some images in the above situations are shown in Figure. 4. Bluish images' example lies on first row, and greenish images' example lies on second row, the yellowish underwater image is in the third row, the low-illuminated underwater image is in the fourth row, and the shallow water image is in the fifth row.

The results showed that our model achieves excellent results in a variety of situations. During different color backgrounds, our model can fully retain the appearance characteristic of objects while successfully restoring the ground truth color background. Our proposed model has an excellent performance in blue, green, yellow underwater images, as well as images from shoal water. However, our proposed model does not have the best performance in low-illuminated underwater images. This indicates that the enhancement effect of the proposed model needs to be improved when a large adjustment for lightness is in demand. In conclusion, the qualitative evaluation shows that our proposed model has achieved excellent results.

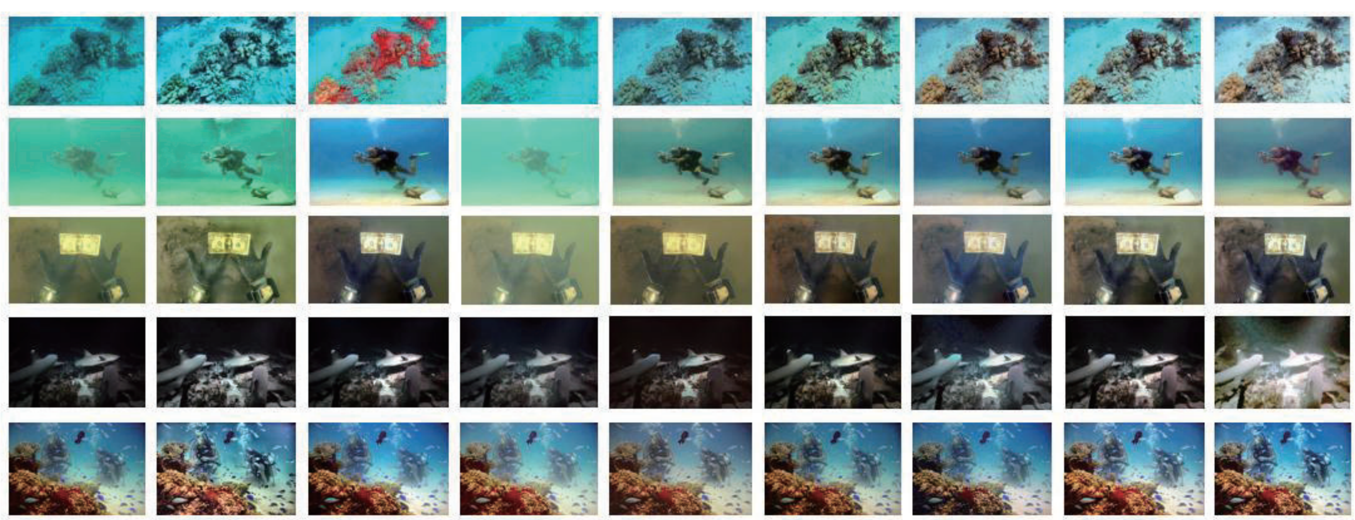

(1)Inputs (2)HB (3)CB (4)NC (5)UWCNN (6)Water-Net (7)UIEC^2-Net (8)Ours (9)Reference

Figure 4. Qualitative evaluation of different situations.

## V. CONCLUSION

During this article, an Improved Water-Net is constructed. Retaining the original backbone network, the inputs are fused by the predicted confidence map. Moreover, the network details are improved by E-Units and Global Softmax. Experiments demonstrate that our proposed network achieves excellent results. From quantitative analysis, our proposed model performmed the best in our evaluated underwater image enhancement methods. According to qualitative analysis, our proposed model does not have the best performance in low-illuminated underwater images but has an excellent performance in other images from distinct styles. Considering the need to preprocess the input images to obtain the HE, WB and GC images, original images cannot be directly enhanced. In future work, we will hold on to make research about enhancement, make image enhancement be input by a single image. Meanwhile, we will hold on to optimizing the neural network architecture to improve image enhancement effect. Moreover, our proposed method will be applied to Autonomous Underwater Vehicles to play an important role in practical engineering problems.

## REFERENCES

[1] Khatib, Oussama, et al. "Ocean One: A Robotic Avatar for Oceanic Discovery." IEEE Robotics & Automation Magazine, vol. 23, no. 4, pp. 20–29, 2016

[2] Carreras, Marc, et al. "Sparus II AUV-A Hovering Vehicle for Seabed Inspection." IEEE Journal of Oceanic Engineering, vol. 43, no. 2, pp. 344–55, 2018

[3] Zhao, Zhenxi, et al. "Composited FishNet: Fish Detection and Species Recognition From Low-Quality Underwater Videos." IEEE Transactions on Image Processing, vol. 30, pp. 4719–34, 2021

[4] C. Li, C. Guo, W. Ren, R. Cong, J. Hou, S. Kwong, and D. Tao, "An underwater image enhancement benchmark dataset and beyond," *IEEE Transactions on Image Processing*, vol. 29, pp. 4376–4389, 2019.

[5] S. G. Narasimhan and S. K. Nayar, "Contrast restoration of weather degraded images," *IEEE Trans. Pattern Anal. Mach. Learn*., vol. 25, no. 6, pp. 713–724, 2003.

[6] T. Treibitz and Y. Y. Schechner, "Active polarization descattering," *IEEE Trans. Pattern Anal. Mach. Intell.*, vol. 31, no. 3, pp. 385–399, 2009.

[7] H. Li, X. Wang, T. Bai, W. Jin, Y. Huang, and K. Ding, "Speckle noise suppression of range gated underwater imaging system," *Proc. SPIE*, vol. 38, no. 18, pp. 3937–3944, 2009.

[8] Z. Murez, T. Treibitz, R. Ramamoorthi, and D. Kriegman, "Photometric stereo in a scattering medium," in *Proc. IEEE Conf. Comput. Vis. Pattern Recognit. (CVPR)*, vol. 39, no. 9, pp. 3415–3423, 2015

[9] C. Ancuti, C. O. Ancuti, T. Haber, and P. Bekaert, "Enhancing under water images and videos by fusion," in *Proc. IEEE Conf. Comput. Vis. Pattern Recognit. (CVPR)*, pp. 81–88, 2012

[10] R. Dhivya and R. Prakash and M. R. Mohanraj. "Color Balance and Fusion for Underwater Image Enhancement". *Digital Image Processing,* vol. 27, no. 1, pp. 25-29, 2019

[11] Stark J A. "Adaptive image contrast enhancement using generalizations of histogram equalization," *IEEE transactions on image processing : a publication of the IEEE Signal Processing Society,* vol. 9, no. 5, pp. 889-96, 2000

[12] Virgil E. Vickers. "Plateau equalization algorithm for real-time display of high-quality infrared imagery". *Optical Engineering*, vol. 35, no. 7, pp. 1921-1927, 1996

[13] Zuiderveld K, " Contrast Limited Adaptive Histogram Equalization," Graphic Gems IV. San Diego: Academic Press Professional, pp. 474 — 485, 1994

[14] Shi Y, Yang J, Wu R, "Reducing Illumination Based on Nonlinear Gamma Correction," *IEEE International Conference on Image Processing,* vol. 1, pp. 529-532, 2007

[15] Huafeng Li et al. "Infrared and visible image fusion scheme based on NSCT and low-level visual features". *Infrared Physics and Technology*, vol. 76, pp. 174-184, 2016

[16] K. Iqbal, M. Odetayo, A. James, R. A. Salam, and A. Z. H. Talib, "Enhancing the low quality images using unsupervised colour correction method," in *Proc. IEEE Int. Conf. Syst., Man Cybern.*, 2010, pp. 1703–1709

[17] Gao Shao-Bing et al, "Underwater Image Enhancement Using Adaptive Retinal Mechanisms," *IEEE transactions on image processing: a publication of the IEEE Signal Processing Society*, vol. 28, no. 11, pp. 5580-5595, 2019

[18] HU Haokun, CAO Wei, YUAN Jieyu, et al, "A low-illumination image enhancement algorithm based on morphological-Retinex(MR) operator", *IEEE/ACIS 6th International Conference on Big Data, Cloud Computing, and Data Science*, Zhuhai, 2021, pp. 66-72.

[19] S. Zhang, T. Wang, J. Dong, and H. Yu, "Underwater image enhancement via extended multi-scale retinex," *Neurocomputing*, vol. 245, no. 5, pp. 1–9, 2017.

[20] Chen Wei et al. "Deep Retinex Decomposition for Low-Light Enhancement." 2018.

[21] K. He, J. Sun, and X. Tang, "Single image haze removal using dark channel prior," *IEEE Trans. Pattern Anal. Mach. Intell.*, vol. 33, no. 12, pp. 2341–2353, 2011.

[22] P. Drews-Jr, E. R. Nascimento, S. S. C. Botelho, and M. F. M. Campos, "Underwater depth estimation and image restoration based on single images," *IEEE Comput. Graph. Appl.*, vol. 36, no. 2, pp. 24–35, 2016.

[23] Y.-T. Peng, K. Cao, and P. C. Cosman, "Generalization of the dark channel prior for single image restoration," *IEEE Trans. Image Process.*, vol. 27, no. 6, pp. 2856–2868, 2018.

[24] Li, Chongyi, Saeed Anwar, and Fatih Porikli. "Underwater Scene Prior Inspired Deep Underwater Image and Video Enhancement." *Pattern recognition*, vol. 98, p. 107038, 2020

[25] Wang, Yudong, Jichang Guo, Huan Gao, and Huihui Yue. "UIEC^2-Net: CNN-Based Underwater Image Enhancement Using Two Color Space." *Signal processing. Image communication*, vol. 96, p. 116250–, 2021

[26] Chen L and Ding D D. 2022. "Joint multi-residual learning for underwater image enhancement". *Journal of Image and Graphics,* vol. 27, no. 5, pp. 1577-1588, 2022

[27] CHEN X L, et al. "Underwater image enhancement algorithm combining deep learning and image formation model" .*Computer Engineering*, vol. 48, no. 2, pp. 243-249.2022

[28] Wu, Junjun, et al. "FW-GAN: Underwater Image Enhancement Using Generative Adversarial Network with Multi-Scale Fusion." *Signal Processing. Image Communication*, vol. 109, p. 116855–, 2022.

[29] Panetta, Karen, et al. "Comprehensive Underwater Object Tracking Benchmark Dataset and Underwater Image Enhancement With GAN." *IEEE Journal of Oceanic Engineering*, vol. 47, no. 1, pp. 59–75,, 2022.

[30] Lan, Zeru, et al. "An Optimized GAN Method Based on the Que-Attn and Contrastive Learning for Underwater Image Enhancement." *PloS One*, vol. 18, no. 1, pp. e0279945–e0279945, 2023.

[31] Xu, Huipu, et al. "UUGAN: a GAN-Based Approach Towards Underwater Image Enhancement Using Non-Pairwise Supervision." *International Journal of Machine Learning and Cybernetics*, vol. 14, no. 3, pp. 725–38, 2023.

[32] Liu, Risheng, Xin Fan, Ming Zhu, Minjun Hou, and Zhongxuan Luo. "Real-World Underwater Enhancement: Challenges, Benchmarks, and Solutions Under Natural Light." *IEEE transactions on circuits and systems for video technology*, vol. 30, no. 12, pp. 4861–4875, 2020

[33] D. Berman, D. Levy, S. Avidan, and T. Treibitz, "Underwater single image color restoration using haze-lines and a new quantitative dataset," *arXiv,* p. *1811.01343, 2018*

[34] H. Zhao, O. Gallo, I. Frosio, and J. Kautz, "Loss functions for image restoration with neural networks," IEEE Transactions on computational imaging, vol. 3, no. 1, pp. 47–57, 2016.

[35] Zhou Wang, Bovik, A. ., Sheikh, H. ., & Simoncelli, E. . . Image quality assessment: from error visibility to structural similarity. IEEE Transactions on Image Processing, vol. 13, no. 4, pp. 600–612, 2004.